J. Phys. II France **7** (1997) 295–304 FEBRUARY **1997**, PAGE 295

Phase Separation in Polymer Solutions Induced by Shear

Akira Onuki (*), Ryoichi Yamamoto and Takashi Taniguchi

Department of Physics, Kyoto University, Kyoto 606-01, Japan

(Received 19 August 1996, received in final form 21 October 1996, accepted 5 November 1996)

PACS.83.50.Fc – Linear viscoelasticity
PACS.64.70.Ja – Liquid-liquid transitions

Abstract. — We numerically investigate nonlinear regimes of shear-induced phase separation in entangled polymer solutions. Use is made of a time-dependent Ginzburg-Landau model describing two fluid dynamics of polymer and solvent. As a new dynamic variable a conformation tensor is introduced to represent chain deformations. Above the coexistence curve a dynamical steady states is attained, where fluctuations are enhanced on various spatial scales. At relatively large shear elongated polymer-rich regions form a transient network supporting most of the stress. Because such a network is continuously deformed in shear flow, the shear stress and the normal stress difference exhibit large fluctuations.

In two component viscoelastic fluids the network stress can act on the two components asymmetrically. Then there arises dynamical coupling between stress and diffusion leading to a number of intriguing viscoelastic effects. Most spectacular is shear-induced phase separation in semidilute polymer solutions, in which light scattering can be drastically enhanced even above the coexistence temperature $T_{\rm cx}$ [1–6]. In this system the composition fluctuations give rise to inhomogeneities of the network structure and the applied shear produces stress imbalance resulting in diffusion in the direction of phase separation. Theoretically this effect was first examined to linear order in the composition fluctuation $\delta\phi$ on the assumption that the polymer stress instantaneously follows $\delta\phi$ [7]. Formal time-dependent Ginzburg-Landau theories have also been developed [8–12], in which a tensor variable $\overleftrightarrow{W}$ is introduced to represent chain deformations and viscoelasticity. In this scheme we set up dynamic equations in which the composition and $\overleftrightarrow{W}$ are coupled. Hence the time scales of these two variables can be comparable. As their first applications, if the dynamic equations are linearized around homogeneous states, they can describe non-exponential decay of the composition fluctuations in dynamic light scattering [13], viscoelastic effects in early stage spinodal decomposition [14], and the fluctuation enhancement in shear in the linear regime [10–13]. However, it is very difficult to solve the dynamic equations in nonlinear regimes and there is no satisfactory understanding of the physical mechanisms in phase separation with or without shear. The aim of this paper is to investigate the nonlinear regime of shear-induced phase separation by numerically solving the dynamic equations. Viscoelastic effects in spinodal decomposition of deeply quenched polymer solutions are investigated in another paper [15].

(*) Author for correspondence (e-mail: onuki@ton.scphys.kyoto-u.ac.jp)

We briefly set up a dynamic model of an entangled polymer solution in the semidilute regime, $\phi > \phi_c = N^{-1/2}$ and $\phi \ll 1$, ϕ_c being the critical volume fraction and N being the polymerization index. In terms of the polymer volume fraction ϕ and the conformation tensor $\overleftrightarrow{W} = \{W_{ij}\}$, the free energy is given by [10]

$$F\{\phi, \overleftrightarrow{W}\} = \int d\mathbf{r}\left[f(\phi) + \frac{1}{2}C(\phi)|\nabla\phi|^2 + \frac{1}{4}G(\phi)\sum_{ij}(W_{ij} - \delta_{ij})^2\right] . \quad (1)$$

Here $f(\phi) \cong (k_B T/v_0)\left[\phi \ln \phi/N + (\frac{1}{2} - \chi)\phi^2 + \frac{1}{6}\phi^3\right]$ is the Flory-Huggins free energy density [16], where v_0 is the volume of a monomer and χ is the so-called interaction parameter dependent on the temperature. In the second term $C(\phi) \propto 1/\phi$ from the scaling theory. The last term of (1) is the elastic energy of the network, $G(\phi)$ being the shear modulus. For simplicity we assume that the deviation of $\overleftrightarrow{W}$ from the equilibrium value $\overleftrightarrow{I}$ (= the unit tensor) is small, so the elastic free energy is bilinear in $\overleftrightarrow{W} - \overleftrightarrow{I}$. Because $\overleftrightarrow{W}$ represents the network deformation, its motion is determined by the polymer velocity $\mathbf{v}_p$ and its simplest dynamic equation is of the form [10],

$$\frac{\partial}{\partial t}W_{ij} + (\mathbf{v}_p \quad \nabla)W_{ij} - \sum_k (D_{ik}W_{kj} + W_{ik}D_{jk}) = -\frac{1}{\tau(\phi)}(W_{ij} - \delta_{ij}) , \quad (2)$$

where $D_{ij} = \partial v_{pi}/\partial x_j$ is the gradient tensor of the polymer velocity $\mathbf{v}_p$. The left hand side of (2) is called the upper convective time derivative in the rheological literature [17] and $\tau(\phi)$ is the stress relaxation time very long in the semidilute region [18]. From (1) and (2) we may calculate free energy changes against infinitesimal motion of the network to obtain the network stress in the form [8–12],

$$\overleftrightarrow{\sigma}_p = 2\overleftrightarrow{W} \cdot (\delta F/\delta \overleftrightarrow{W}) = G(\phi)\overleftrightarrow{W} \cdot (\overleftrightarrow{W} - \overleftrightarrow{I}) . \quad (3)$$

In particular, in weak, homogeneous, and stationary flow, (2) is solved to give $W_{ij} - \delta_{ij} \cong \tau(D_{ij} + D_{ji})$. In shear flow we require $|W_{xy}| < 1$ for the validity of (1), which is also the condition of the Newtonian regime $\dot{\gamma}\tau < 1$, where $\dot{\gamma}$ is the shear rate. The solution viscosity in the Newtonian regime is $\eta_p = G(\phi)\tau(\phi)$, which is supposed to be much larger than the solvent viscosity η_0. For rapid motions, on the other hand, our system behaves as a gel and $W_{ij} - \delta_{ij} \cong \partial u_{pi}/\partial x_j + \partial u_{pj}/\partial x_i$, where $\mathbf{u}_p$ is the time integral of $\mathbf{v}_p$ and has the meaning of the displacement of the network.

Note that the solvent velocity $\mathbf{v}_s$ and the polymer velocity $\mathbf{v}_p$ are different when the diffusion is taking place. The volume fraction is convected by $\mathbf{v}_p$ as

$$\frac{\partial}{\partial t}\phi = -\nabla \cdot (\phi \mathbf{v}_p) . \quad (4)$$

On the other hand, the average velocity $\mathbf{v} = \phi\mathbf{v}_p + (1 - \phi)\mathbf{v}_s$ obeys the usual hydrodynamic equation,

$$\bar{\rho}\frac{\partial}{\partial t}\mathbf{v} = -\nabla p_1 - \nabla \cdot \overleftrightarrow{\Pi} + \eta_0 \nabla^2 \mathbf{v} , \quad (5)$$

where $\bar{\rho}$ is the average mass density and the stress tensor $\overleftrightarrow{\Pi} = C(\phi)(\nabla\phi)(\nabla\phi) - \overleftrightarrow{\sigma}_p$ arises from the gradient term in (1) and the network stress. For simplicity we are assuming that the mass densities of the pure polymer and solvent are the same and the fluid is incompressible.

Then the polymer mass composition and the polymer volume fraction coincide and p_1 in (5) is determined from the condition $\boldsymbol{\nabla}\cdot\mathbf{v}=0$. Furthermore, assuming that the network stress acts on the polymer and not directly on the solvent, we may derive from a two fluid model [8–12] the equation of the relative velocity $\mathbf{w}=\mathbf{v}_{\rm p}-\mathbf{v}_{\rm s}$,

$$\bar{\rho}\phi\frac{\partial}{\partial t}\mathbf{w}=-\zeta(\phi)\mathbf{w}-\phi\,\boldsymbol{\nabla}\frac{\delta F}{\delta\phi}+\,\boldsymbol{\nabla}\cdot\overleftrightarrow{\sigma}_{\rm p}+\frac{1}{4}G(\phi)\,\boldsymbol{\nabla}\sum_{ij}(W_{ij}-\delta_{ij})^2\,, \tag{6}$$

where $\zeta(\phi)$ is the friction coefficient of order $6\pi\eta_0 b^{-2}\phi^2$, b being the monomer size. For slow motions we may set $\partial\mathbf{w}/\partial t=0$ in (6); then, $\mathbf{w}$ is expressed in terms of ϕ and $\overleftrightarrow{W}$. Furthermore neglecting the last term of (6), we obtain the expression $\mathbf{w}=\zeta(\phi)^{-1}(-\phi\,\boldsymbol{\nabla}\delta F/\delta\phi+\,\boldsymbol{\nabla}\cdot\overleftrightarrow{\sigma}_{\rm p})$ appearing in the literature [7, 10–14], which implies that stress imbalance ($\boldsymbol{\nabla}\cdot\overleftrightarrow{\sigma}_{\rm p}\neq 0$) gives rise to diffusion (stress-diffusion coupling). Note that the last term of (6) is small compared to the third term on the right hand side for small deviations of $\overleftrightarrow{W}$. It is written in (6) to ensure the nonnegative-definiteness of the heat production rate [10]. That is, without externally imposed flow, we can check $-{\rm d}\mathcal{F}/{\rm d}t\geq 0$ for any disturbances from (1) $\sim$(6), where $\mathcal{F}=F\{\phi,\overleftrightarrow{W}\}+\frac{1}{2}\int{\rm d}\mathbf{r}\bar{\rho}\mathbf{v}^2$ is the total free energy. Therefore, the system tends to a homogeneous equilibrium state with $\overleftrightarrow{W}-\overleftrightarrow{I}=\mathbf{v}=\mathbf{w}=0$ as $t\to\infty$ if there is no macroscopic flow.

We numerically solve the above equations in two space dimensions on a 128×128 square lattice by applying a shear flow $\langle v_x\rangle=\dot{\gamma}y$ and $\langle v_y\rangle=0$, at $t=0$. In this paper we report results for

$$\langle\phi\rangle/\phi_{\rm c}=2,\qquad T=T_{\rm c}\quad\text{or}\quad\chi-1/2=N^{-1/2}\,, \tag{7}$$

where $\langle\cdots\rangle$ is the spatial average. Note that the solution is above the coexistence curve. The coefficient of the gradient free energy in (1) is written as $C(\phi)=(k_{\rm B}T/v_0)C_0/\phi$, where $C_0=b^2/18$ in the random phase approximation [16]. In terms of the thermal correlation length $\xi=(NC_0/5)^{1/2}$($\sim$ the gyration radius) and the cooperative diffusion constant $D_{\rm co}$ [16] in the state (7) in the absence of shear, we measure space and time in the units of $\ell=(5/3)^{1/2}\xi$ and $\tau_0=2.5\ell^2/D_{\rm co}$. We also set $G(\phi)=(k_{\rm B}T/v_0)\phi^3$ and $\tau(\phi)=0.3\tau_0[(\phi/\phi_{\rm c})^4+1]$. The solvent viscosity is taken to be $\eta_0=(k_{\rm B}T/v_0)\phi_{\rm c}^3\tau_0$, which is equivalent to assume $\zeta(\phi)=\eta_0\phi^2/C_0$. Then the Newtonian solution viscosity and the relaxation time are written as $\eta_{\rm p}(\phi)/\eta_0=\Phi^3\tau(\phi)/3\tau_0$ and $\tau(\phi)/\tau_0=0.3(\Phi^4+1)$ in terms of $\Phi=\phi/\phi_{\rm c}$, which yield $\eta_{\rm p}/\eta_0=13.6$ and $\tau/\tau_0=5.1$ in the initial state (7). In our case the shear modulus $G(\phi)$ is considerably larger and the relaxation time $\tau(\phi)$ is much smaller than in the experiments [4–6] for the computational convenience. Furthermore, our functional forms of $G(\phi)$ and $\tau(\phi)$ are not well consistent with the experiment in theta solutions [18] and scaling theories of polymer solutions in theta solvent [19, 20], but we believe that the essential feature is insensitive to the detailed forms of $G(\phi)$ and $\tau(\phi)$.

While there are only small thermal fluctuations in equilibrium, shear can enlarge the thermal fluctuations on small spatial scales ($\gtrsim$ the mesh size ℓ in the following simulations) in an early stage ($t<\dot{\gamma}\tau_0$). In later times the fluctuations on various spatial scales appear and the system tends to a strongly fluctuating, dynamical steady state. Hence random source terms in the dynamic equations are indispensable for this effect, though they have been omitted so far for simplicity. In fact, if the initial values $\phi(x,y,0)$ are random numbers distributed around the average $\langle\phi\rangle$ and there are no random source terms in the dynamic equations for $t>0$, the fluctuations initially grow but eventually disappear as $t\to\infty$. In our simulations we therefore add Gaussian random source terms on the right hand sides of (2), (5), and (6), which are related to $1/\tau$, η_0, and ζ, respectively, to satisfy the fluctuation-dissipation

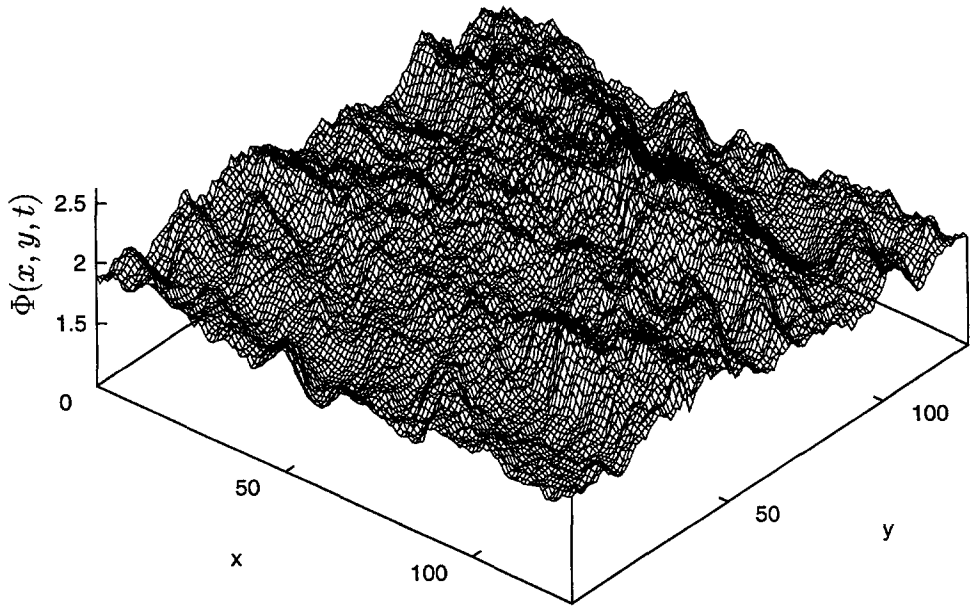

Fig. 1. — $\Phi(x,y,t) = \phi(x,y,t)/\phi_c$ at $t = 500$ for $\dot{\gamma}\tau_0 = 0.02$. The space coordinates are measured in the units of $\ell = (5/3)^{1/2}\xi$, ξ being the correlation length in equilibrium. The x axis is along the flow direction and the y axis is along the shear direction.

relations. After the dynamic equations are made dimensionless, these random source terms are still proportional to a parameter $\epsilon = [v_0 N^{3/2}/\ell^d]^{1/2}$, which has not yet been specified, d being the spatial dimensionality. Our model is self-consistent for arbitrary ϵ, so we set $\epsilon = 0.1$ in our simulations. The variance $\sigma = [\langle(\Phi - \langle\Phi\rangle)^2\rangle]^{1/2}$ taken over all the lattice points is then equal to 0.038 in equilibrium ($\dot{\gamma} = 0$). Furthermore for slow disturbances we are allowed to set $\partial \mathbf{v}/\partial t = \partial \mathbf{w}/\partial t = 0$ in (5) and (6). Then $\mathbf{v}$ can be expressed in terms of $\overleftrightarrow{\sigma}_p$ and the random stress tensor using the FFT scheme.

First, we show results for $\dot{\gamma}\tau_0 = 0.02$ or $\dot{\gamma}\tau_0 = 0.10$. in terms of τ in the initial state (7). Figure 1 displays $\Phi(x,y,t) = \phi(x,y,t)/\phi_c$ at $t = 500$, where $\sigma = 0.162$ and $|W_{xy}| \lesssim 0.2$. We can see fluctuations on various spatial scales. Figure 2 illustrates snapshots of the fluctuations, where the darkness represents $(\Phi(x,y,t) - \Phi_{min})/(\Phi_{max} - \Phi_{min})$, $\Phi_{max} = 2.675$ and $\Phi_{min} = 1.087$ being the maximum and the minimum of $\Phi(x,y,t)$ at these times. Here the fluctuations are elongated in abnormal directions, which are opposite to those in sheared near-critical fluids without elasticity [21,22], as the linear calculations have shown [7,10–13]. Furthermore we can see that the largest scale fluctuations are continuously deformed by hydrodynamic convection on the time scale of $1/\dot{\gamma}\tau_0 (= 50)$. The structure factor $S(q_x, q_y, t)$ is much enhanced at small q but is fluctuating in time, so in Figure 3 we show the time average of the structure factor taken over the time interval $150 < t < 1000$. It is the butterfly scattering pattern observed in the scattering experiment [4–6].

Secondly, we show results for $\dot{\gamma}\tau_0 = 0.05$ or $\dot{\gamma}\tau = 0.25$ in terms of τ in the initial state (7). Figure 4 displays $\Phi(x,y,t)$ at $t = 400$, where $\sigma = 0.549$ and the fluctuations are more enhanced than in Figure 1. We also confirm $|W_{xy}| \lesssim 0.5$ here. In spatial regions in which $\Phi(x,y,t)$ deviates considerably below 2, it varies smoothly in space. This is because the small

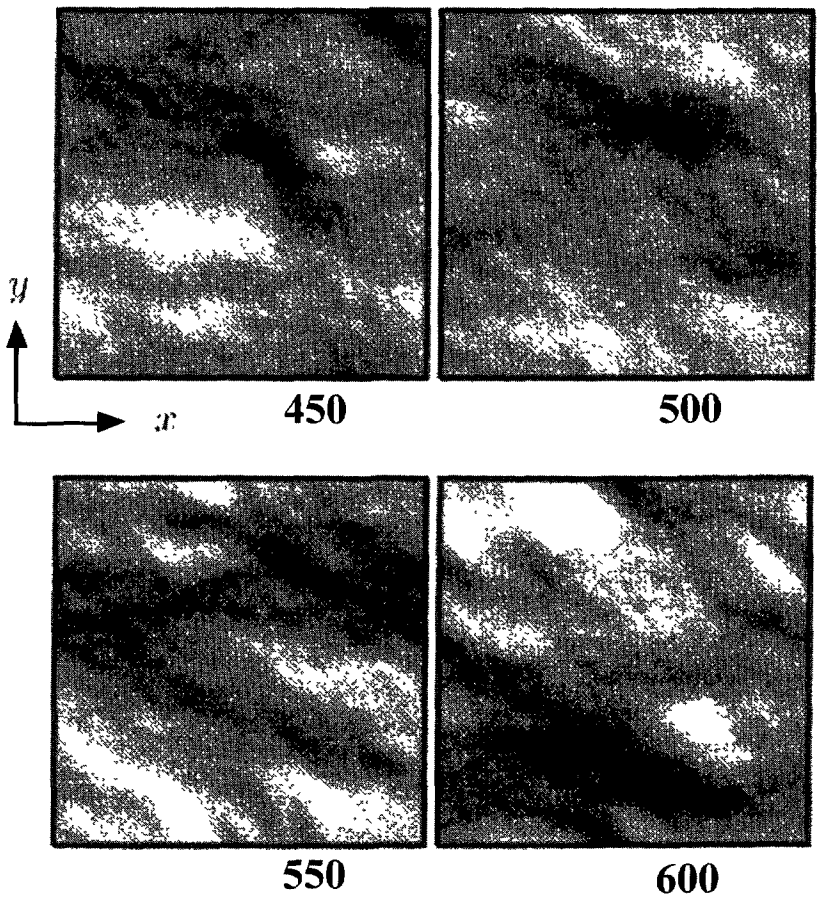

Fig. 2. — Snapshots of $\Phi(x, y, t)$ for $\dot{\gamma}\tau_0 = 0.02$ showing elongation of the fluctuations in abnormal directions. The numbers are the times measured in the units of $\tau_0 = 2.5\ell^2/D_{\rm co}$ after application of shear. The x (flow) direction is horizontal and the y (shear) direction is vertical.

scale fluctuations created by the random source terms do not grow in such regions. On the contrary, in regions where $\Phi(x, y, t) \gtrsim 2$, it varies irregularly even on the mesh size scale ℓ. This is also the case in most spatial regions in the first simulation (see Fig. 1). In Figure 5 we show snapshots of $\Phi(x, y, t)$ as in Figure 2, where $\Phi_{\rm max} = 3.594$ and $\Phi_{\rm min} = 0.380$. Here the polymer-rich regions are elongated into long stripes forming a transient network. Figure 6 shows the time average of the structure factor in the interval $150 < t < 1000$. The peak wave numbers are more smaller and closer to the q_x axis than in Figure 3 in accord with reference [4].

We finally examine the effect of the shear-induced fluctuations on the average shear stress,

$$\sigma_{xy} = \langle \sigma_{{\rm p}xy} \rangle - \langle C(\phi)(\partial\phi/\partial x)(\partial\phi/\partial y) \rangle \ , \tag{8}$$

and the average normal stress difference,

$$N_1 = \langle \sigma_{{\rm p}xx} - \sigma_{{\rm p}yy} \rangle + \langle C(\phi) \Big[(\partial\phi/\partial y)^2 - (\partial\phi/\partial x)^2 \Big] \rangle \ . \tag{9}$$

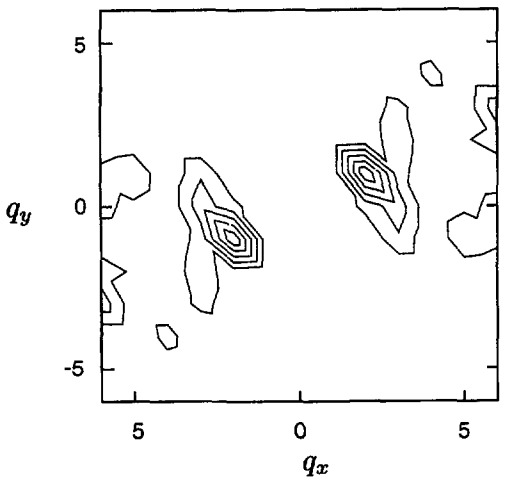

Fig. 3. — Contour plot of the time average of the structure factor for $\dot{\gamma}\tau_0 = 0.02$ in the $q_x - q_y$ plane. The wave vector is measured in the units of $2\pi/128\ell$. The peak height is 15.7.

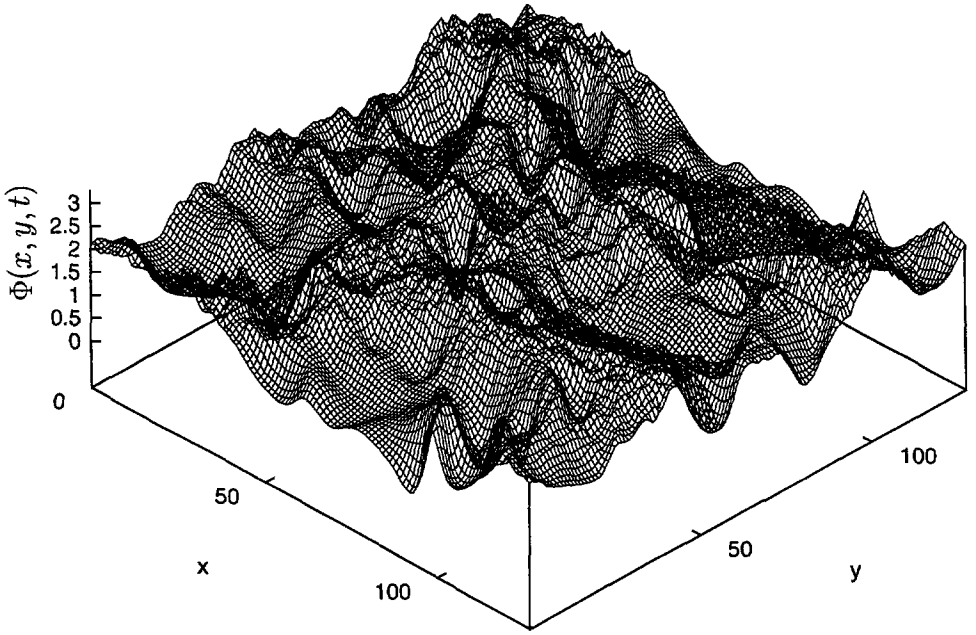

Fig. 4. — $\Phi(x,y,t) = \phi(x,y,t)/\phi_c$ at $t = 400$ for $\dot{\gamma}\tau_0 = 0.05$.

the averages being taken over the lattice points. In our problem we have confirmed that the first terms of (8) and (9) are much larger than the second terms, while the second terms give dominant singular contributions in Newtonian fluids [23]. Figures 7 and 8 display σ_{xy} and N_1 divided by $\eta_0/3\tau_0$ in the time region $0 < t < 800$ for $\dot{\gamma}\tau_0 = 0.01, 0.02$, and 0.05. The shear stress first grows linearly in time ($\propto t$) up to the order of $\eta_p\dot{\gamma}$ at $t \sim \tau$, but it begins to decrease with

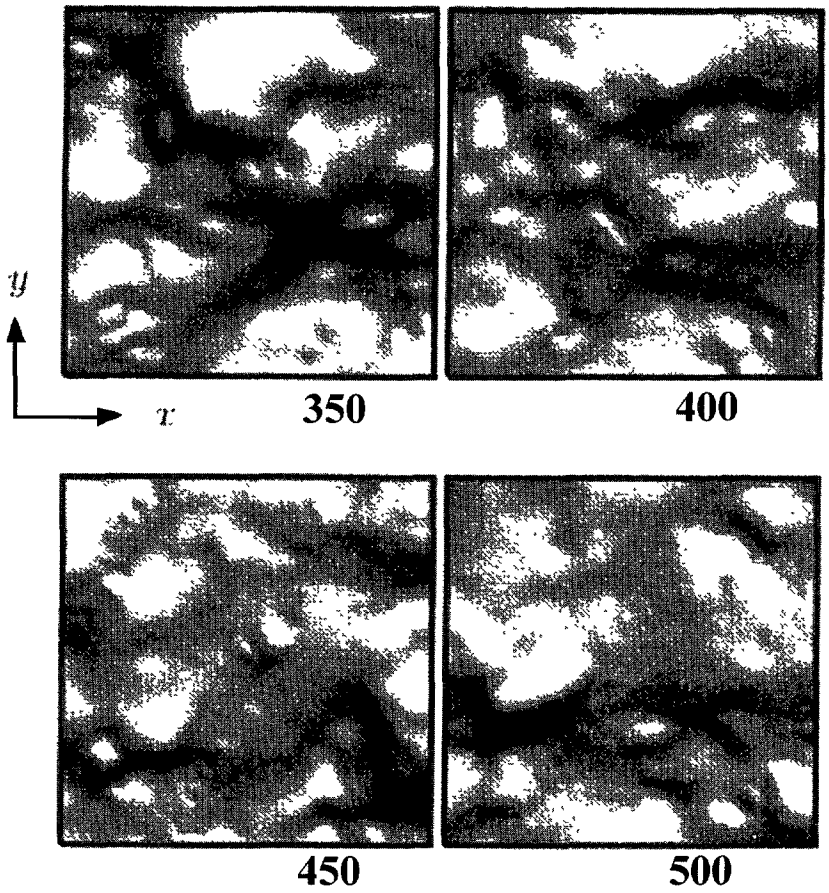

Fig. 5. — Snapshots of $\Phi(x, y, t)$ for $\dot{\gamma}\tau_0 = 0.05$. A network composed of elongated polymer-rich regions is being deformed and destroyed by shear. The x axis is along the flow direction and the y axis is along the shear direction.

growth of the shear-induced fluctuations. The normal stress difference grows as t^2 initially. After the transient stage they both exhibit considerable fluctuations except for the smallest shear $\dot{\gamma}\tau_0 = 0.01$. At the largest shear $\dot{\gamma}\tau_0 = 0.05$, the network composed of elongated polymer-rich regions is often extended throughout the system but is subsequently disconnected. The stress is mostly supported in such a network. This process produces abnormal fluctuations of the stress. Interestingly, in many cases, the normal stress difference takes a maximum (or minimum) when the shear stress takes a minimum (or maximum). In experiments the stress components are measured as the force density acting on a surface with a macroscopic linear dimension d. If d is longer than the characteristic size of the network structure of the polymer-rich region, the temporal stress fluctuations will be suppressed. Nevertheless the shear-induced composition fluctuations will reduce the shear stress on the average and enhance the normal stress difference. Here we mention an early experiment by Lodge [24], who observed abnormal temporal fluctuations of the normal stress difference at a hole of 1 mm diameter from polymer solutions contained in a cone-plate apparatus. He ascribed its origin to the growth

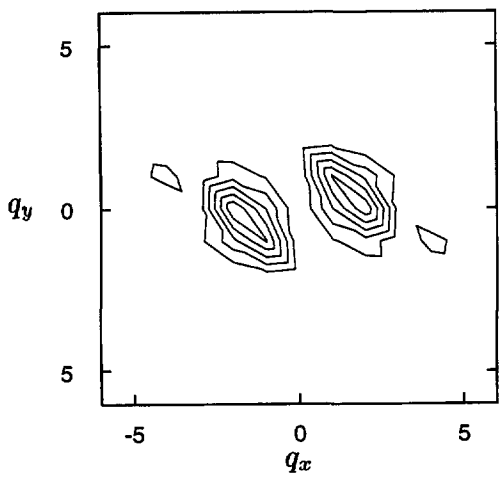

Fig. 6. — Contour plot of the time average of the structure factor for $\dot{\gamma}\tau_0 = 0.05$ in the $q_x - q_y$ plane. The peak height is 470.

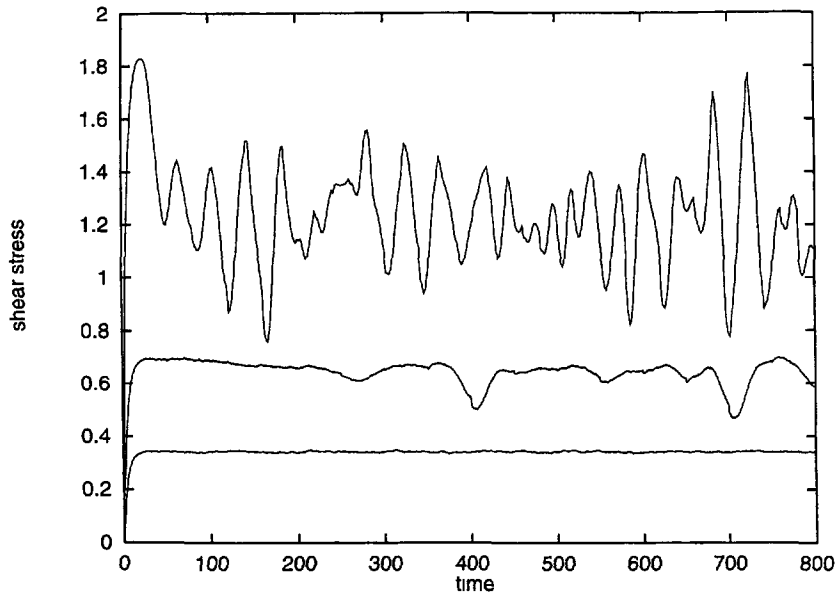

Fig. 7. — Shear stress as a function of time for $\dot{\gamma}\tau_0 = 0.01, 0.02$, and 0.05 from below. The fluctuations become larger with increasing shear.

of inhomogeneities or gel particles of dimensions about 4 mm. We believe that our results are closely related to his observation. Further experiments on small scale stress fluctuations are very informative. Birefringence and dichroism experiments will also be useful.

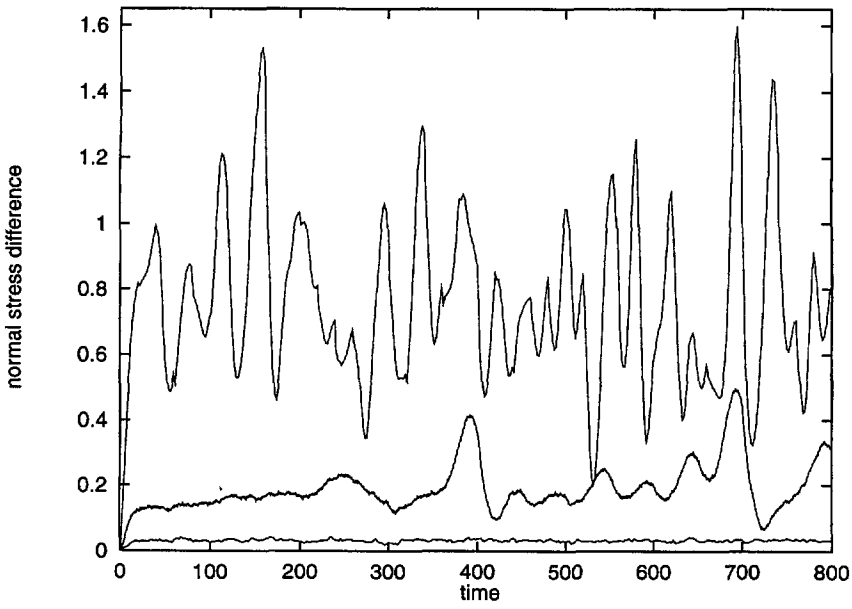

Fig. 8. — Normal stress difference as a function of time for $\dot{\gamma}\tau_0 = 0.01, 0.02$, and 0.05 from below. The fluctuations are even more larger than those of the shear stress.

Our main results are summarized as follows. Although above the coexistence curve, macroscopic phase separation cannot be achieved, the level of the fluctuations increases with increasing shear and can even be comparable to that in spinodal decomposition occurring without shear at lower temperatures. In other words, in the nonlinear regime above the coexistence curve, polymer solutions can undergo *incomplete phase separation* induced by shear. In this dynamically steady state, anisotropic fluctuations grow from small to large scales, but large scale fluctuations are deformed by shear and are eventually dissipated. The random source terms in the dynamic equations are hence indispensable in this cascade process as sources of the growing fluctuations.

Our final remarks are as follows. (i) We will examine the effects below the coexistence curve and in the non-Newtonian regime in a forthcoming paper. We may well expect that the system will phase-separate macroscopically when it is deeply quenched inside the unstable temperature region in the presence of shear. Note also that we have made the shear modulus G larger than in real polymers to have large shear effects even in the Newtonian regime. (ii) It is also worth studying how nucleation is affected by weak shear as it is increased from zero in the metastable temperature region. For near-critical fluids it is established that nucleation can be suppressed if the critical radius becomes smaller than the Taylor break-up size ($\sim \sigma/\eta\dot{\gamma}$, σ being the surface tension) in shear flow [25]. It is unknown how this scenario is changed in polymer solutions. (iii) In asymmetric polymer blends, in which the two polymers have very different viscoelastic properties, the dynamic coupling between stress and diffusion should generally be present [13] as in polymer solutions. In such blends we may predict similar shear-induced composition fluctuations.

References

[1] Ver Strate G. and Philippoff W., *J. Polym. Sci. Polym. Lett.* **12** (1974) 267.
[2] Rangel-Nafaile C., Metzner A.B. and Wissburn K.F., *Macromolecules* **17** (1984) 1187.
[3] Krämer H. and Wolf B.A., *Macromol. Chem. Rapid Commun.* **6** (1985) 21.
[4] Wu X.L., Pine D.J. and Dixon P.K., *Phys. Rev. Lett.* **68** (1991) 2408.
[5] Hashimoto T. and Fujioka K., *J. Phys. Soc. Jpn* **60** (1991) 356; Hashimoto T. and Kume T., *J. Phys. Soc. Jpn* **61** (1992) 1839; Moses E., Kume T. and Hashimoto T., *Phys. Rev. Lett.* **72** (1994) 2037.
[6] van Egmond W., Werner D.E. and Fuller G., *J. Chem. Phys.* **96** (1992) 7742.
[7] Helfand E. and Fredrickson H., *Phys. Rev. Lett.* **62** (1989) 2468.
[8] Grmela M., *Phys. Lett. A* **130** (1988) 81.
[9] Beris A.N. and Edwards B.J., Thermodynamics of Flowing Systems (Oxford University Press, Oxford, 1994).
[10] Onuki A., *Phys. Rev. Lett.* **62** (1989) 2472; *J. Phys. Soc. Jpn* **59** (1990) 3423.
[11] Milner S.T., *Phys. Rev. E* **48** (1993) 3874.
[12] Ji H. and Helfand E., *Macromolecules* **28** (1995) 3869.
[13] Doi M. and Onuki A., *J. Phys. II France* **2** (1992) 1631.
[14] Onuki A., *J. Non-Crystalline Solids* **172-174** (1994) 1151.
[15] Taniguchi T. and Onuki A., *Phys. Rev. Lett.* **77** (1996) 4910.
[16] de Gennes P.G., Scaling Concepts in Polymer Physics, 2nd ed. (Cornell University Press, Ithaca, 1985).
[17] Larson R.G., Constitutive Equations for Poymer Melts and Solutions (Butterworths, Boston, 1986).
[18] Adam M. and Delsanti M., *J. Phys. France* **45** (1984) 1513.
[19] Brochard F. and de Gennes P.G., *Macromolecules* **10** (1977) 1157.
[20] Colby R.H. and Rubinstein M., *Macromolecules* **23** (1990) 2753.
[21] Beysens D., Gbadamassi M. and Moncef-Bouanz B., *Phys. Rev. A* **28** (1983) 2491.
[22] Onuki A. and Kawasaki K., *Ann. Phys. (NY)* **121** (1979) 456; Onuki A., Yamazaki K. and Kawasaki K., *Ann. Phys. (NY)* **131** (1981) 217
[23] Onuki A., *Phys. Rev. A* **35** (1987) 5149.
[24] Lodge A.S., *Polymer* **2** (1961) 195.
[25] Goldburg W.I. and Min K.Y., *Physica A* **204** (1994) 246.